# Optimal control of backwash scheduling for pumping energy saving: Application to the treatment of urban Wastewater

Fatma Ellouze, Yesmine Kammoun, Nesrine Kalboussi, Alain Rapaport, Jérôme Harmand, Samir Nasr, Ben Amar

# Optimal control of backwash scheduling for pumping energy saving: Application to the treatment of urban Wastewater

Fatma Ellouze[a,b,*], Yesmine Kammoun[b,1], Nesrine Kalboussi[c], Alain Rapaport[d], Jérôme Harmand[e], Samir Nasr[f], Nihel Ben Amar[a,b]

[a]Université Tunis El Manar, Ecole Nationale d'Ingénieurs de Tunis, Laboratoire de Modélisation Mathématique et Numérique dans les sciences d'ingénieur, B. P 37 Le Belvédère, 1002 Tunis, Tunisia

[b]Université de Carthage, Institut National des Sciences Appliquées et de Technologie, B. P.676, 1080 Tunis Cedex, Tunisia

[c]Laboratory of Desalination and Nature Water Valorization, Centre of Water Researches and Technologies (CERTE), B.P. 273, Soliman 8020, Tunisia

[d]MISTEA, Université Montpellier, INRAE, Institut Agro, Montpellier, France

[e]LBE, Université Montpellier, INRAE, Narbonne, France

[f]National Sanitation Office, 1073 Montplaisir, Tunis, Tunisia

*corresponding author ellouze_fatma@yahoo.fr

[1] current affiliation: Laboratory of Water, Membrane and Environmental Biotechnology, Centre of Water Researches and Technologies (CERTE), B.P. 273, Soliman 8020, Tunisia

**Abstract**

An optimal control strategy for municipal wastewater MBR treatment was applied to investigate its efficiency in minimizing the pumping energy of the system. Based on a simple mathematical model to capture the dynamic evolution of the TransMembrane Pressure (TMP), an optimal switching instant between filtration/backwash was determined to reduce the supplementary pumping energy caused by fouling for a predefined net permeate volume. A MBR pilot treating municipal wastewater was used to generate dynamic data of TMP. The pilot was operated with two different strategies: a classical strategy with known operating conditions (10 min filtration and 45s backwash) and an optimal strategy where the frequency was determined based on adjustment of model parameters. Results demonstrated that a satisfactory agreement was achieved between experimental data and model prediction. The optimal strategy was then applied experimentally on the MBR pilot. The two strategies were compared in terms of energy consumption and fouling degree. The results showed the feasibility of the optimal solution and its reliability to reduce the pumping energy of the system by 7% and decrease residual fouling by 14% compared with a classical strategy.

**Key words**: MBR, fouling, modelling, optimal control of backwash, energy optimization.

## Abbreviation

| | |
|---|---|
| $C$ | solid matter concentration (Kg.m$^{-3}$) |
| $E_{BW}$ | pumping energy consumption during backwash (W.s) |
| $E_f$ | pumping energy consumption during filtration (W.s) |
| $E_T$ | total pumping energy consumption (W.s) |
| $J_{BW}$ | backwash volumetric flux (m$^3$.m$^{-2}$.s$^{-1}$) |
| $J_v$ | permeate volumetric flux (m$^3$.m$^{-2}$.s$^{-1}$) |

| | |
|---|---|
| $k_{1n}$ | hydraulic energy parameters ($m^3$. Pa. $s^{-1}$. $Kg^{-1}$) |
| $k_{2n}$ | hydraulic energy parameters ($m^3$.Pa.$s^{-1}$) |
| $m$ | membrane surface deposited mass ($Kg.m^{-2}$) |
| $\bar{m}$ | deposited mass on singular arc state ($Kg.m^{-2}$) |
| $m_0$ | initial deposited mass ($Kg.m^{-2}$) |
| $q_n$ | volumetric flow during filtration (n:f) or backwash (n:BW) ($m^3.s^{-1}$) |
| $R_{cake}$ | cake resistance ($m^{-1}$) |
| $R_{er}$ | external resistance ($m^{-1}$) |
| $R_{ir}$ | internal resistance ($m^{-1}$) |
| $R_m$ | membrane resistance ($m^{-1}$) |
| $R_{res}$ | residual cake resistance ($m^{-1}$) |
| $TMP$ | Transmembrane Pressure (Pa) |
| $TMP_0$ | transmembrane Pressure at the beginning of each cycle (Pa) |
| $TMP_{01}$ | transmembrane Pressure at the beginning of the first cycle (Pa) |
| $TMP_i$ | transmembrane Pressure at the beginning of the second phase of each cycle (Pa) |
| TSS | Total suspended Solid ($Kg.L^{-1}$) |
| $u$ | flux direction control |
| $\bar{u}$ | flux direction control at singular arc state |
| $V$ | permeate collected volume ($m^3$) |
| $V^*$ | target volume at the end of optimal control strategy ($m^3$) |
| $\bar{V}$ | collected volume at the end of singular arc |
| $V_e$ | Collected volume at the beginning of singular arc |
| $\alpha$ | specific cake resistance ($m.Kg^{-1}$) |
| $\beta$ | parameters related to the shear force ($m^2.Kg^{-1}$) |
| $\eta$ | backwash efficiency ($s^{-1}$) |
| $\mu$ | Viscosity (Pa.s) |

## 1. Introduction

Due to the global water scarcity, there is increasing interest in developing and optimizing advanced technologies for appropriately treating wastewater for recycling purposes. Membrane bioreactors have been extensively studied for wastewater treatment due to their ability to produce high-quality effluent, occupy a small footprint, and reduce sludge production [1,2]. This technology combines an activated sludge and membrane filtration process to achieve high nutrient removal and complete biomass rejection without the need for secondary settling. However, membrane fouling remains a major challenge in MBRs as it reduces permeation flux when filtration operates at a constant transmembrane pressure (TMP) or increases TMP in constant flux mode. This results in a decrease of effluent quality and an increase in operating costs [3, 4].

At full scale, physical cleaning methods such as relaxation, backwash, and aeration are commonly employed to limit clogging. However, this phenomenon is complex and depends on several operational parameters, including flux, filtration and backwash duration, and aeration flow [5]. Without an optimal cleaning strategy, the process may suffer from inefficient filtration performance, resulting in high energy consumption and low water recovery [6, 7]. Several studies have focused on optimizing MBR operating conditions to mitigate clogging [8, 9]. In this context, significant progress has been made in developing more efficient fouling control methods.

An effective backwash strategy can delay irreversible fouling and reduce the overall cost associated with UF foulants [10-12]. Backwash duration and frequency are important parameters [13-15] that influence fouling and cannot be determined solely based on the supplier's recommendations [16]. Most MBR plants operate at a constant flux, and fouling is generally indicated by an increase in transmembrane pressure (TMP) over time. Therefore, a higher backwash duration and frequency can cause a net production loss without necessarily reducing the fouling rate. On the other hand, infrequent backwashing can increase the build-up rate of internal fouling and lead to increased energy consumption. Thus, there is a compromise to be found that can be computed provided that a model is available, and an optimal control is well defined. The novel challenge is to operate MBRs at optimal operating parameters, in a sense to be clearly defined, that allow for good water productivity at minimal energy cost.

A variety of control and optimization methods have been proposed for better management of backwash sequences. However, many of these studies are just based on empirical investigations [11, 13, 17-19]. For example, Hwang *et al.* [18] proposed a power-type empirical correlation between irreversible filtration resistance and the filtration cycle to select optimal backwash conditions. Gonzalez *et al.* [20] proposed a feedback control using an empirical fouling model to adjust permeate flux as a function of filtration length and the maximum permissible TMP during a cycle. However, more advanced control methods that use mathematical models to anticipate the dynamic behavior of the process and adapt the cleaning strategy are emerging in the literature [21-25]. For instance, optimal control approaches have been developed recently to design optimal backwash strategies and maximize filtration system performance. Cogan *et al.* [21, 22] and Kalboussi *et al.* [24, 25] applied Pontryagin's Maximum Principle (PMP) to predict the optimal instants of switching between filtration and backwash periods that maximize the net water production over a given operating time of a membrane filtration process operating at constant TMP. They demonstrated numerically that the optimal strategy significantly improves the net permeate production [24]. With respect to previously mentioned empirical strategies, optimal controls synthesized on the basis of mathematical models present the advantage of guaranteeing their optimality.

It is interesting to note that while many studies have focused on developing optimal control strategies for separation systems operating at a constant transmembrane pressure, more recent studies have focused on developing optimal control strategies for constant flux filtration systems, which are typical in real-world MBR applications. For example, Cogan *et al.* [26] developed a model to calculate an optimal balance between filtration and backwash to maximize water production efficiency while considering the effects of membrane aging during full scale potable reuse. They showed that used model compares well with the full-scale operational data, and model parameters accurately capture the fouling kinetics with membrane age, providing clues to changes in optimal backwash timing and duration. On the other hand, Aichouch *et al.* [27] used a simple mathematical model to develop an optimal backwash scheduling strategy that minimized pumping energy consumption for a predefined volume production. This work seems interesting since the increase in TMP induced by biofouling can represent 30 to 70% of energy consumption [28] but this optimal approach was simply tested in simulation and never implemented at pilot scale.

The objective of this paper is therefore to conduct an experimental implementation of the optimal control backwash as developed in Ref. [27], to reduce pumping energy consumption in a constant flux MBR. To the best of our knowledge, the practical implementation of theoretical optimal strategies has not yet been undertaken. This study can provide valuable insights into the real effectiveness of this approach in mitigating fouling and reducing pump energy consumption. The findings from such experiments can contribute to the development of more efficient fouling control

methods and improve the overall performance and sustainability of MBR processes. Steps of this work consist first in validating the simple model to capture the dynamic behavior of the MBR, then in synthesizing the optimal control strategy according to the data gained from model analysis and finally in evaluating and discussing the practical implementation of the optimal strategy compared to the classical one.

## 2. Experimental section

### 2.1 SMBR pilot system

The experimental study was carried out using a ZeeWeed submerged membrane bioreactor pilot ZW10 (Fig. 1) installed in the wastewater treatment plant WWTP of Charguia (Tunis, Tunisia). The SMBR is equipped with a hollow fiber membrane (M), from Polymem-France. The membrane has pores diameter of 0.01 µm, filtration surface area of 1.5 $m^2$ and is immersed in a cylindrical biological tank of 220 L (T2). Biological treatment was performed under aerobic conditions with compressed air introduced in the aeration pipes (A) around the membrane module. The air flow rate measured with a rotameter (F1) was fixed at 2 CFM in the reactor to maintain the dissolved oxygen above 1.5 mg/L and create a shear for fouling mitigation.

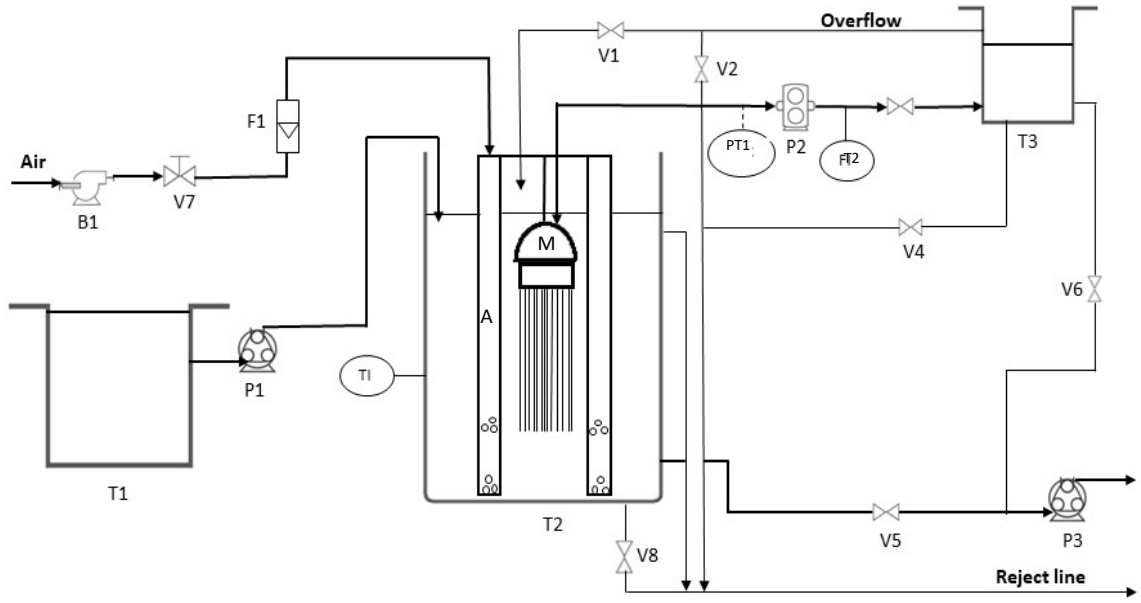


FIG. 1: Experimental set up of Zenon SMBR ZW10

A: aeration pipes, B1: blower, F1: float flowmeter, FT2: reversible flow magnetic transmitter M: Hollow fiber membrane, P1: feed pump, P2: reversible gear permeate pump, P3: sludge pump, PT1: pressure transmitter, V: valve, T1: feed tank, T2: bioreactor, T3: permeate tank

The permeate was continuously extracted from the top of the membrane module by reversible micro-gear pump P2 (micropump serie GJ) connected to a programmable automate system (siemens SIMATIC HMI). The automation system allowed for the control of the pump's rotation speed and the ability to reverse the pump's rotation during backwash phase.

The experiments were carried out at constant permeate flux regulated by the gear pump P2. The transmembrane pressure was recorded every 10 s using PT1 pressure transmitter. The flow rates of both

permeate and backwash were measured by a reversible magnetic flow transmitter FT2 (Kobold). The sludge was extracted from the bottom of the aeration tank T2 using a peristaltic pump P3.

### 2.2 Operating conditions

The peristaltic pump P1 was used to feed continuously the bioreactor with the real sewage from the Charguia WWTP aeration tank T1. Table 1 summarizes the feed sewage characteristics. The experiments were conducted during the June-July period, no significant change in the feed composition nor in the climatic conditions was observed throughout this period.

Table 1: Characteristics of sewage used to feed the SMBR

| Water quality parameter | Mean value |
|---|---|
| pH | 6.8 |
| Conductivity ($\mu S.cm^{-1}$) | 3745 |
| TSS ($g.L^{-1}$) | 2.2 |
| COD ($mgO_2.L^{-1}$) | 371 |
| $BOD_5$ ($mgO_2.L^{-1}$) | 286 |
| MVS ($g.L^{-1}$) | 1.8 |

The SMBR was first operated in the classical mode. Then, the operation of the process was switched in the optimal control mode. In the classical mode, a periodical backwash of 45s was applied every 10 min of filtration as recommended by commercial suppliers [29]. The backwash was initiated by reversing the direction rotation of the permeate pump (P2). The optimal control mode considered in this study will be detailed in the optimal control section 4.

The permeate flux was kept constant at $8.5 \pm 0.5$ $L.m^{-2}.h$, below the critical flux determined by flux step method [30]. Whereas the backwash flux was two times much higher. To keep the bioreactor level constant, the feed and the permeate were circulated at the same flowrates. The sludge extraction rate was fixed at 0.6 L/h which correspond to a sludge retention time (SRT) of 15 days [29].

### 2.3 Analytical methods

Water samples were taken at the inlet (T1) and outlet (T3) of the bioreactor. Chemical oxygen demand COD, biochemical oxygen demand BOD and total suspend solid TSS analyzes were carried out immediately after sampling.

The TSS was measured by gravimetric methods with 0.7 µm filter for influent and 0.45 µm filter for permeate samples. COD were determined using WTW kits and WTW photolab S6 photometer. The BOD5 was measured according to European Standard Method with WTW Oxitop system.

## 3. Fouling characterization

Registered *TMP* data were analyzed according to "resistance in series" model (Eq.1) to characterize membrane fouling.

$$TMP = \mu J_v(R_m + R_{cake} + R_{res}) \quad (1)$$

$\mu$ is the permeate viscosity, $J_v$ is the volumetric permeate flux, $R_m$ is the clean membrane resistance, $R_{cake}$ is the reversible fouling resistance and $R_{res}$ is the residual fouling resistance. As described in [9], the residual fouling can be divided into internal fouling resistance ($R_{ir}$) related to pore blocking or attached

matter that is not eliminated during backwash and external fouling resistance ($R_{er}$) linked to fouling layer recompression.

$$R_{res} = R_{ir} + R_{er} \quad (2)$$

$R_{ir}$ can be calculated by *Eq.3*.

$$TMP_0 = \mu J_v (R_m + R_{ir}) \quad (3)$$

where $TMP_0$ is the transmembrane pressure just at the beginning of each cycle (Fig.2).

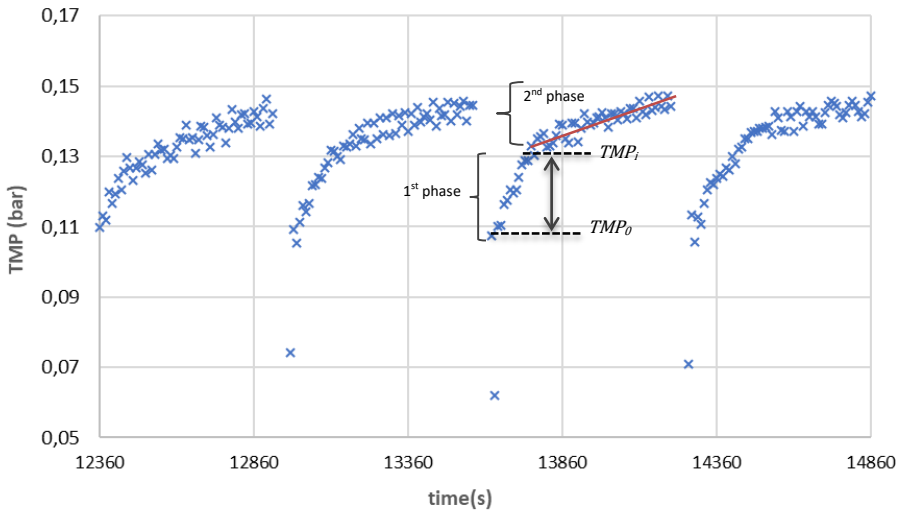


Fig.2 : TMP profile of filtration/backwash cycles for the classical control mode (10min filtration and 45s backwash). $TMP_0$ is TMP just at the beginning of each cycle and $TMP_i$ is the initial TMP in the second phase of each cycle

External fouling resistance correspond to the sudden increase of the TMP in the beginning of each cycle due to the rapid recompression of the external layer (first phase, Fig.2). Its value can be deduced from Eq.2-Eq.4.

$$TMP_i = \mu J_v (R_m + R_{res}) \quad (4)$$

$TMP_i$ is the initial transmembrane pressure in the second phase of each cycle where the TMP starts to increase linearly with filtration time (Fig.2) [9].

However, reversible fouling resistance is associated to the cake layer deposition and can be calculated by *Eq.1*.

## 4. Modelling and optimal control Section

### 4.1 Fouling Model description

The used model was developed in a previous work [31]. It is based on mass balance for a dead-end filtration operating at constant flux and aims to simulate the TMP variation during filtration and

backwash phases by considering cake building, pore blocking and cake porosity decrease. For the needs of this study, the model was simplified to only consider the reversible clogging by cake layer.

During the filtration phase, the mass accumulated over time on the membrane surface ($m$) is assumed to be the difference between the mass deposited by convective forces and the mass detached by shear forces generated by the aeration in the biological tank:

$$\frac{dm}{dt} = f_f(m) = C.J_v - C.J_v.\beta.m \quad (5)$$

where $C$ is the suspended matter concentration, $J_v$ the permeate volumetric flux and $\beta$ a parameter related to the shear force.

During backwash, the mass deposited on the membrane surface decreases as follows:

$$\frac{dm}{dt} = f_{BW}(m) = -\eta\,.m \quad (6)$$

where $\eta$ is the backwash efficiency.

If we consider a control $u$ that takes, by convention values 1 during filtration and -1 during backwash, the accumulated mass deposited on the membrane surface can be written as follows:

$$\frac{dm}{dt} = \frac{1+u}{2} f_f(m) + \frac{1-u}{2} f_{BW}(m) \quad (7)$$

According to the resistance in series model, by neglecting the residual fouling, the TMP, can be expressed as:

$$TMP = \mu\ J_v\ (R_m + R_{cake}) \quad (8)$$

$R_{cake}$ is proportional to the specific cake resistance α as:

$$R_{cake} = \alpha\, m \quad (9)$$

In this study, MATLAB 2014b software was used for simulation and process optimization. Model validation and parameters identification were realized by fitting the normalized experimental data ($TMP/TMP_{01}$) to the theoretical normalized ones by the least squares method using Matlab fmincon function, defined as an optimization function. The model efficiency was evaluated by determining the regression coefficient $R^2$as a performance indicator, calculated by the following expression:

$$R^2 = 1 - \frac{\sum_{j=1}^{N}\left(TMP_j - TMP_{pj}\right)^2}{\sum_{j=1}^{N}\left(TMP_j - TMP_{av}\right)^2} \quad (10)$$

where $TMP_e$, $TMP_p$ and $TMP_{av}$ were the experimental, predicted and average transmembrane pressures, respectively. $j$ is the measure number and $N$ is the total number of measures.

**4.2 Optimal control approach**

As described in Ref. [27], an optimal control problem was developed to minimize the pumping hydraulic energy using a mathematical model describing the process. The control signal *u(t)* is adjusted based on feedback which is dependent on the accumulated mass $m$ and the produced volume $V$. Pontryagin's

Maximum Principle (PMP) was the mathematical tool applied to determine the analytical solution of the optimal control problem. The fundamental contribution of optimal control theory is that the applied theoretical tools provided by the PMP enable the calculation of an optimal accumulated mass value, $\bar{m}$, that minimizes the total hydraulic energy consumed by MBR pump to produce a predefined volume $V^*$.

The total produced volume $V$ is defined as:

$$dV = \int_0^T \left(\frac{1+u}{2} J_v - \frac{1-u}{2} J_{BW}\right) dt \quad (11)$$

Where $J_{BW}$ is the backwash flux and $T$ is the time for which the target permeate volume $V^*$ is reached.

The pumping energy demand $E_T$ during a time interval [0, $T$] depends on the deposited mass $m$ as:

$$E_T = \int_0^T \left(\frac{1+u}{2} . E_f(m) + \frac{1-u}{2} . E_{BW}(m)\right) dt \quad (12)$$

$E_f$ and $E_{BW}$ are respectively the required pumping energy during filtration and backwash phases.

$E_f$ and $E_{BW}$ can be calculated using *Eq. 1*3.

$$E_n = q_n \; TMP_n \quad (13)$$

Where $q$ is the flowrate and the index $n$ refers to f during filtration and BW for backwash phase.

From Eq. 8 and 9, $E_n$ can be rewritten in terms of the attached mass $m$:

$$E_n = k_{1n}\, m + k_{2n} \quad (14)$$

$k_{1n}$ and $k_{2n}$ are parameters relatives to the hydraulic energy their expressions are represented in table 2.

Table 2 : Hydraulic energy parameters expressions during filtration and backwash

| Parameter | Expression | |
|---|---|---|
| $k_{1n}$ ($m^3$. $Pa$. $s^{-1}$. $Kg^{-1}$) | $\frac{q_n^2}{A}\, \mu\, \alpha$ | *(15)* |
| $k_{2n}$ ($m^3$.$Pa$.$s^{-1}$) | $\frac{q_n^2}{A}\, \mu\, R_m$ | *(16)* |

*$n$ refers to f during filtration and BW for backwash phase

The optimal solution depends on the state of membrane fouling and is summarized in [27] as:

$$u(m,V) = \begin{cases} +1, \; if \; m < \bar{m} \\ \bar{u}, \; if \; m = \bar{m} \quad and \quad V \le \bar{V} \\ +1, \; if \; m > \bar{m} \quad and \quad V > \bar{V} \end{cases} \quad (17)$$

In Eq. 17, $\bar{m}$, $\bar{V}$ and $\bar{u}$ are the control parameters and depend on the parameters of the fouling model described previously. The procedure for calculating $\bar{m}$, $\bar{V}$ and $\bar{u}$ is summarized in Appendix.

A schematic diagram of the optimal solution is represented in Fig 3.

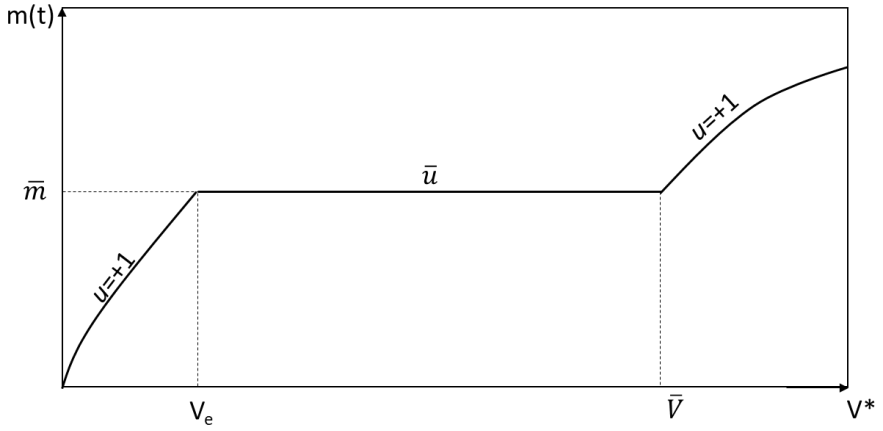


Figure 3: Schematic representation of the optimal control solution developed in [27]

As we consider that the membrane is initially clean ($m_0 = 0$), the optimal solution begins with $u = 1$ until m reaches $\bar{m}$ corresponding to $V = V_e$. Then, in a second phase, $[V_e, \bar{V}]$, a constant control $\bar{u}$ called singular arc is applied to maintain the mass of the cake layer around $\bar{m}$ until the switching volume $\bar{V}$ is reached. $\bar{u}$ takes value between [-1, 1]. Finally, for the last phase $[\bar{V}, V^*]$, it is optimal to finish the process with filtration cycle ($u = 1$) until the target volume $V^*$.

It should be noted that the total operating time of the process depends on the target volume $V^*$. Contrary to $\bar{V}$, the others control parameters $\bar{m}$, $\bar{u}$ and $V_e$ are independent on $V^*$ and remain unchanged whatever the total operating time.

Fig. 3 presents the general optimal control synthesis for the problem considered. Notice that for some initial conditions, the optimal control consists in switching from -1 to +1 instead of staying on the singular arc [27]. In practice, this case is very particular and, in most cases, it may be neglected, notably as long as V* is large enough.

For the singular arc, the control signal $\bar{u}$ takes an intermediate value between -1 and 1. However, in practical applications, implementing this exact value is not feasible. Nevertheless, it is possible to approximate the theoretical optimum by alternating between -1 and 1 in a way that keeps the mass $m$ close to $\bar{m}$. This approximation is detailed in section practical implementation section 5.4.

## 5. Results and discussion

### 5.1 Water treatment efficiency

Samples of influents and effluents were taken from the SMBR system. Parameters such as TSS, COD and $BOD_5$ were analyzed, and mean values are summarized in table 3. It can be noted that the applied strategy didn't affect the effluent quality. The slight deviations observed are mainly due to fluctuations of the influent quality.

Table 3 : influent and effluent characteristics and removal efficiency

| | Influent ($mg.L^{-1}$) | Effluent ($mg.L^{-1}$) | Removal efficiency (%) |
|---|---|---|---|
| TSS | 2100 ± 84 | 6 ± 2 | 99 |
| COD | 250 ± 10 | 51 ± 10 | 80 |
| BOD | 240 ± 20 | 9 ± 3 | 96 |

The influent COD was around 250 $mgO_2.L^{-1}$, while the permeate had a lower COD concentration of less than 51$mgO_2.L^{-1}$, resulting in COD removal efficiency of approximately 80%. The COD rejection could probably be improved to reach higher value by varying the operating conditions, like increasing the SRT, but it was not the aim of this study. The DBO rejection rate was higher, reaching 97%. Nonetheless, the rejection rates are considered satisfactory and comparable to those reported in Ref. [32]. Regarding total suspended solid TSS, a high rejection rate was observed (more than 99%). The permeate contained only trace amounts of suspended matter, below 8 $mg.L^{-1}$.

### 5.2 Model calibration and parameters estimation

For model validation, the theoretical data were compared to the experimental normalized TMP data registered for classical experience. The model parameters determined experimentally are presented in Table 4. Others model parameters (table 5) were identified using least square method as described in model description section. As the used membrane was not new, an initial deposed mass $m_0$ = 6. $10^{-3}$ $kg.m^{-2}$ was considered as the initial condition. $R_m$ was determined experimentally from pure water permeability and C, the suspended solid concentration, was considered as the TSS concentration in the biological reactor.

Table 4 : Experimental model parameters

| **Parameters** | **Value** |
|---|---|
| $J_v$ ($m^3.m^{-2}.s^{-1}$) | 2.71 $10^{-6}$ |
| $J_{BW}$ ($m^3.m^{-2}.s^{-1}$) | 5.66 $10^{-6}$ |
| $PTM_{01}$ (Pa) | 7892.4 |
| $R_m$ ($m^{-1}$) | 1.79 $10^{+12}$ |
| $C$ ($Kg.m^{-3}$) | 2184 $10^{-3}$ |

Table 5 : Model parameters identified by least squares method

| **Parameters** | **Value** |
|---|---|
| $\beta$ ($m^2.kg^{-1}$) | $10^{-6}$ |
| $\alpha$ ($m.kg^{-1}$) | 2.02 $10^{+14}$ |
| $\eta$ ($s^{-1}$) | 4.9 $10^{-3}$ |

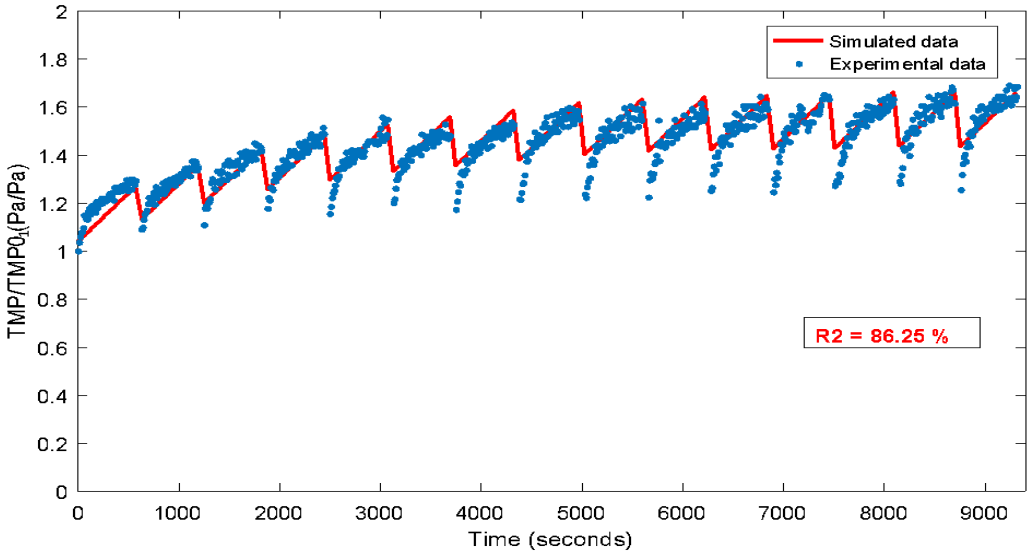


Figure 4 : Model fitting with experimental data obtained for the classical strategy

The comparison of model simulation and experimental normalized data shows satisfactory fitting with an important coefficient regression 86.25 % (Fig.4). The discrepancy observed is mainly due to hypothesis assuming no irreversible fouling in the model. In fact, from Fig.4, it can be observed that the model fit mainly the linear rise of the TMP corresponding to cake fouling.

Despite its simplicity, the proposed model reproduces in satisfactory way the experimental TMP of the classical experience. Hence, the identified model parameters can now be used for computing the optimal control.

As the main objective of this study is the minimization of the permeate pump hydraulic energy $E_T$, the parameters ($k_{1i}$ et $k_{2i}$) related to the energy were calculated according to the equations 14 and 15 and represented in table 6.

Table 6 : Pumping Energy parameters values

| **Parameters** | **Value** |
|---|---|
| $k_{1f}$($m^5$. Pa. $s^{-1}$. $Kg^{-1}$) | 2.0769 |
| $k_{2f}$($m^3$. Pa. $s^{-1}$) | 0.0185 |
| $k_{1BW}$($m^5$. Pa. $s^{-1}$. $Kg^{-1}$) | 9.0551 |
| $k_{2BW}$($m^3$. Pa. $s^{-1}$) | 0.0807 |

### 5.3 optimal control strategy

To evaluate the efficiency of the optimal solution, the optimal control parameters ($\bar{m}$, $\bar{V}$ and $\bar{u}$) were calculated with the identified model parameters (α and β) using the appropriate mathematical design model (*cf.* Appendix). The target volume $V^*$ was chosen equal to 0.04 $m^3.m^{-2}$ corresponding approximatively to the volume collected after 5h of operation with the classical strategy. Fig.5-A and B shows theoretical optimal solution of the control (u) and the deposed mass (m) on the membrane, respectively, as a function of the volume produced for a predefined volume $V^*$= 0.04 $m^3.m^{-2}$.

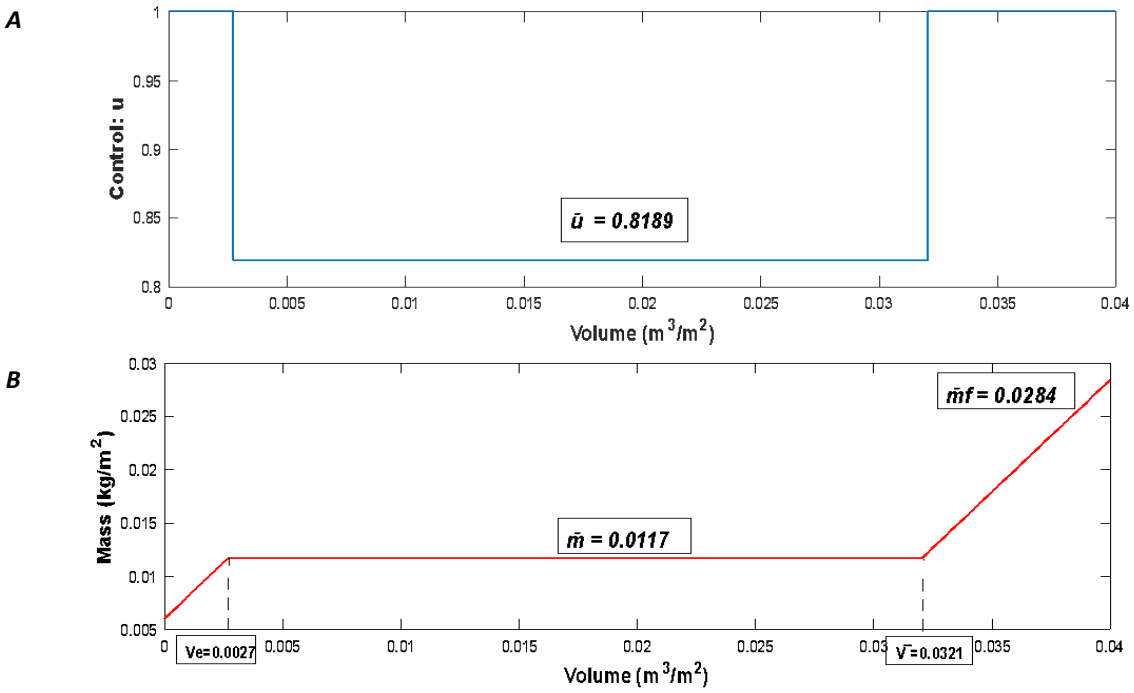


Figure 5 : (A) The theoretical optimal operating strategy over $V^*$ = 0.04 $m^3/m^2$; (B) The corresponding mass accumulated on the membrane surface.

As the initial condition $m_0$ = 6 $10^{-3}$ kg/$m^2$ is less than $\bar{m}$ = 1.17 $10^{-2}$ kg.$m^{-2}$, our system operates initially in filtration ($u$ = 1) up to a volume $V_e$ = 0.0027 $m^3$.$m^{-2}$ corresponding to a filtration time of 16 min. Once the required mass at the surface of the membrane reaches the value $\bar{m}$, the singular control $\bar{u}$ is applied until reaching the volume $\bar{V}$ = 0.0321 $m^3$.$m^{-2}$. The value of ū in this case study is equal to 0.8189. The cake mass ($m$) was maintained at $\bar{m}$ during the singular arc volume interval [$V_e$, $\bar{V}$] which corresponds to a filtration/backwash duration of 4 hours and 12min. A final filtration cycle ($u$ = 1) for 48 min is set up when $V$= $\bar{V}$. Fig.5 shows that the durations of the first and last cycle are shorter compared to the time spent on the singular arc defined by $m(t)$ = $\bar{m}$. Filtration times corresponding to the collected volumes $V_e$, $\bar{V}$ and $V^*$ were calculated using *Eq.11*.

This optimal solution was simulated with Matlab to estimate theoretically the pump energy consumption for a targeted volume of 0.04$m^3$.$m^{-2}$. Fig. 6 represents the evolution of simulated $E_T$ for the classical and optimal strategies.

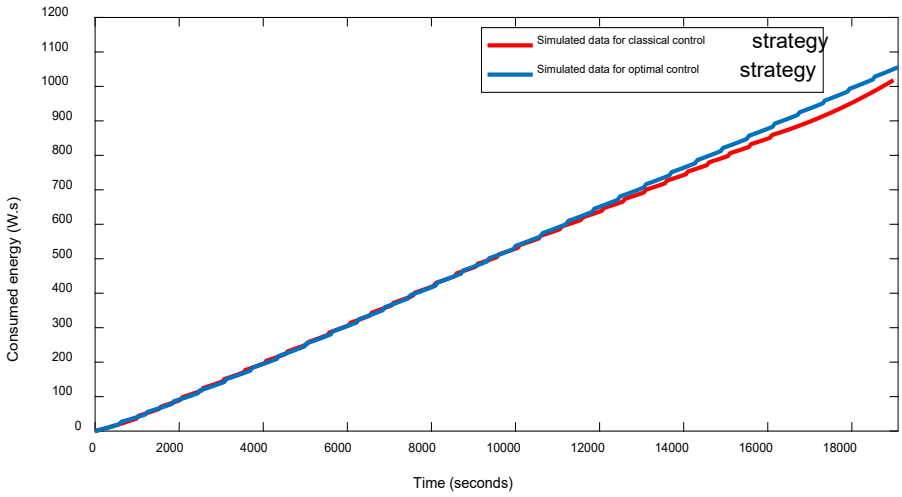


Figure 6: Simulated hydraulic pump energy for the classical and optimal strategy

As shown in Fig.6, the model predicts an energy consumption of 1056 W.s when simulating data of classical strategy to collect $V^*$ = 0.04 $m^3.m^{-2}$. However, the optimal strategy requires less energy consumption of about 1042 W.s compared to the classical one. The gap between both consumption is observed from about 12000s and became more pronounced over time filtration.

At this stage, the optimal solution has no physical signification as in the singular arc $\bar{u}$ is different from 1 and -1. In the next section, an approximation of the optimal solution is constructed to convert $\bar{u}$ = 0.8189 into filtration ($u$ = 1) and backwash periods ($u$ = -1).

### 5.4 Practical implementation

To approximate $\bar{u}$ only by filtration and backwash cycles, such that $m$ remains close to $\bar{m}$ during the singular arc interval time, we consider that $\bar{u}$ represents the ratio between the net time production and total time cycle as:

$$\bar{u} = \frac{t_f - t_{BW}}{t_f + t_{BW}} \qquad (18)$$

$t_f$ and $t_{BW}$ represent respectively the filtration and backwash duration in each cycle.

The latter expression means that if $\bar{u}$ = 1, then all the cycle time will be spent in filtration ($t_{BW}$ = 0) and if $\bar{u}$ = –1, the cycle time will be spent in backwash ($t_f$ = 0).

Based on *Eq.18*, filtration and backwash times can be calculated during the singular arc interval $[V_e, \bar{V}]$. The backwash period was kept the same as the classical strategy *i.e* 45s to compare the performance of the classical and optimal strategies experimentally. In this case, the filtration time was 7.5 min corresponding to a commutation number between filtration and backwash equal to 32.

The optimal strategy sequence which will be applied experimentally is summarized in Fig. 7.

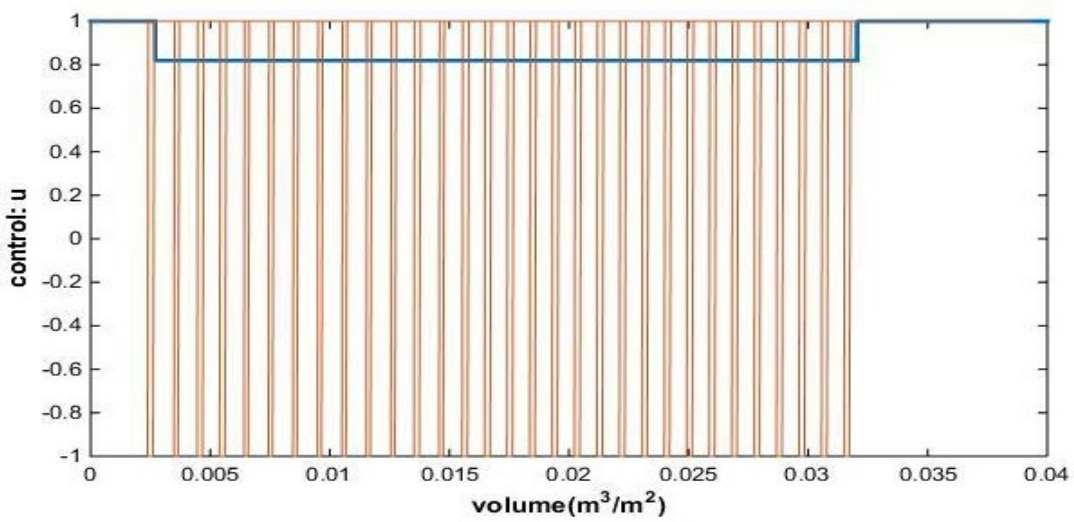


Figure 7: the adapted strategy to be carried out during the singular arc

### 5.5 Classical vs optimal strategy

Adapted optimal strategy (Fig.7) was applied on the SMBR, and the experimental results were analyzed in terms of fouling and hydraulic pump energy consumption then compared to the classical strategy data.

#### 5.5.1 Fouling characterization

TMP analysis provides information on reversible (cake layer) and residual clogging as described in experimental section. The calculated resistance $R_t$, $R_{cake}$, $R_{res}$, $R_i$ and $R_e$ are shown in Fig 8 for classical and optimal experiences.

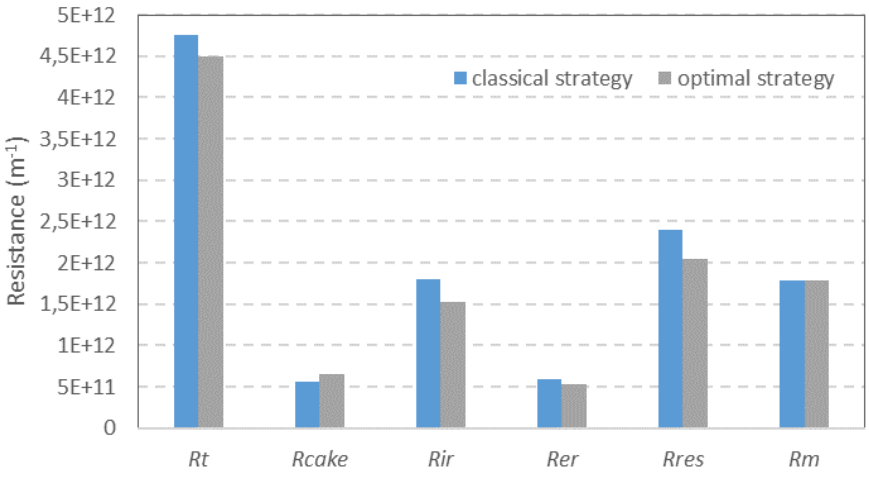


Figure 8: Different hydraulic resistances for classical and optimal strategy

Fig.8 illustrates some differences in the fouling profile of classical and optimal experiences. The total hydraulic resistance is slightly higher for the classical experience than the optimal one. For both strategies the residual fouling exceeds reversible fouling which is in concordance with the works of

Jiang et *al.* and Vera *et al.* [9, 33]. They showed [9] that the magnitude of the residual resistance is greater than the reversible resistance due to pore blocking. Based on the $R_{ir}$ and $R_{er}$ results, the residual fouling caused by pore blocking and particles adsorption was more intensive than that caused by the external layer recompression.

Moreover, it can be observed that $R_{res}$ is higher for classical experience than the optimal one. The residual resistance for the classical experience contributes to 50% of the total resistance against 45% for optimal experience. McAdam *et al.* [34] reported on a dead-end filtration MBR applied to groundwater that it exists a critical cycle duration, associated to a critical mass deposition, beyond which the physical cleaning is less efficient, and so the residual fouling increased. During the singular arc for the optimal strategy, $\bar{m}$ is probably closer to the critical mass so the physical cleaning is more performant reducing the residual fouling. Likewise, $R_{cake}$ is more important for optimal experience ($6.54\ 10^{+11}\ m^{-1}$) than classical one ($5.63\ 10^{+11}\ m^{-1}$). In fact, for the optimal experience, the first and last filtration cycles are longer than the classical experience. Longer filtration time favors cake layer deposition which can protect the membrane surface against pore blocking.

#### 5.5.2 Hydraulic pump energy consumption

The optimal strategy was applied experimentally on SBMR and the TMP data were used to calculate the pump hydraulic energy during filtration and backwash sequences (*Eq.13*).

Fig. 9-A and -B shows, respectively, the collected permeate volume and the pumping energy consumed for the two experiences.

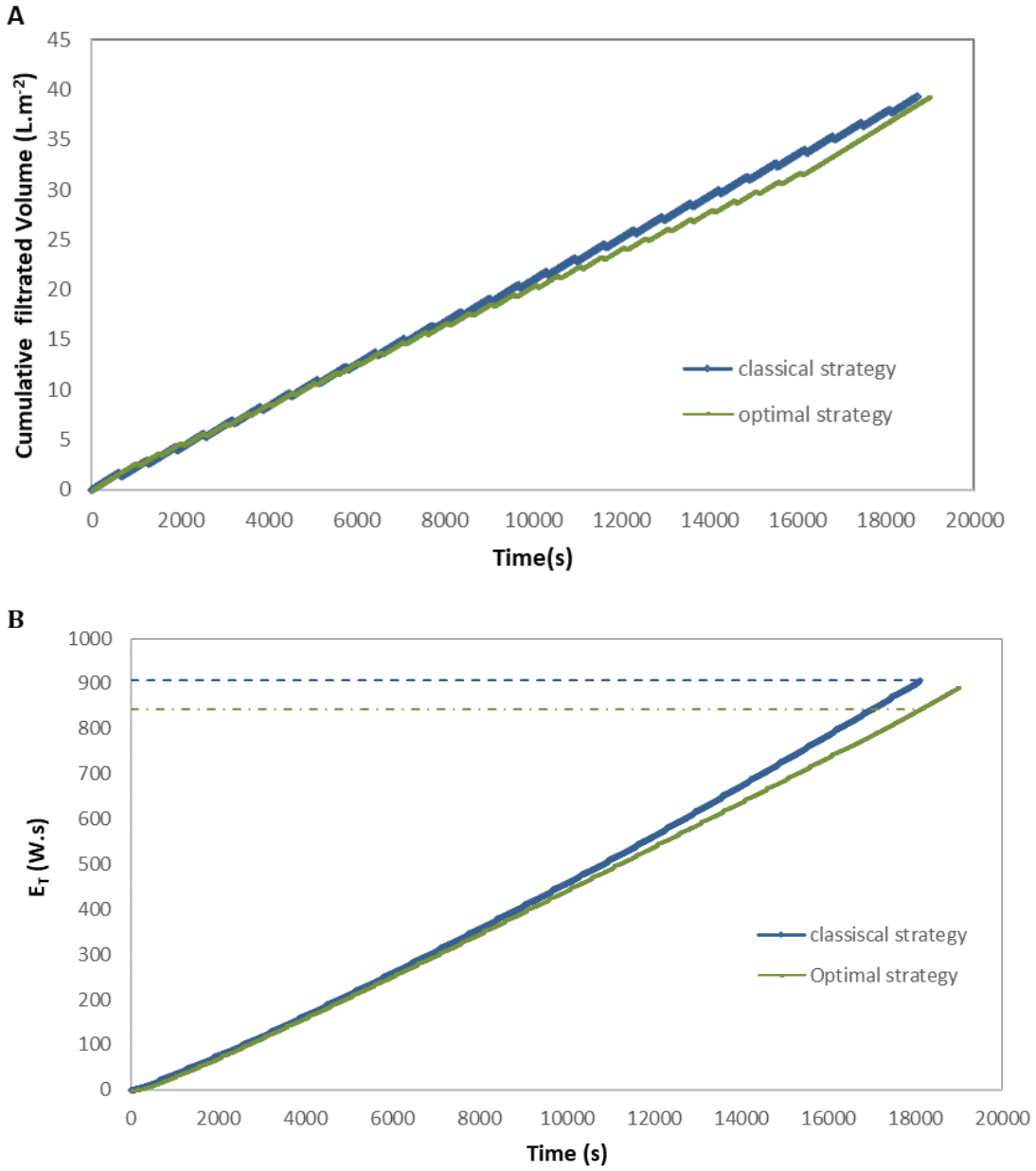


Figure 9: (A) Cumulative permeate volume ($L.m^{-2}$) and (B) Cumulative Hydraulic pumping energy consumption for classical and optimal strategy over time. The blue and green dotted lines (in B) correspond respectively to the energy consumption to produce a net volume of 0.037 $m^3.m^{-2}$ for classical and optimal strategy

Although the optimal control approach applied in this study does not consider productivity as an optimization criterion, it is noteworthy that the total time required to collect the same volume from both experiments is quite similar, as seen from Fig. 9-A. The net permeate flux of the optimal experiment is 7.46 $L.m^{-2}.h^{-1}$ which is slightly lower than that of the classical experience at 7.57 $L.m^{-2}.h^{-1}$. However, it is interesting to observe that the optimal strategy has effectively reduce the total consumed hydraulic pump energy compared to the classical strategy (Fig.9-B). For the same net permeate produced of 0.0373 $m^3.m^{-2}$, corresponding to 18 110 seconds of operation, the classical strategy requires a total hydraulic energy of 907 W.s with 749 W.s consumed during filtration. However, the optimal strategy consumes only 892 W.s (730 W.s during filtration) to produce 0.0393 $m^3.m^{-2}$ of net permeate. For the same volume

produced 0.0373 $m^3.m^{-2}$, a 7% reduction in consumed hydraulic pump energy is realized when the optimal strategy is applied.

One important point to note is that the optimal control strategy consumes less hydraulic energy during filtration, even though it spends more time on the filtration operation (94% of the time versus 93% for the classical strategy). This indicates that the optimal strategy effectively reduces membrane clogging. In conclusion, the optimal strategy provides direct benefits for MBR operation by reducing pumping energy consumption and indirect benefits by preserving the membrane against fouling. This, in the longer term, could lead to a reduction in additional expenses incurred by membrane cleaning and/or replacement.

## 6. Conclusion

MBR is a promising technology for municipal wastewater treatment however fouling control remains the main challenge to decrease the operational cost of the system. In this study, an optimal control backwash strategy was applied to a MBR to decrease the supplementary operational cost of pumping induced by fouling. A simple mathematical model is used to capture the dynamic behavior of the system in order to arrive at suitable optimal strategy. The simple used model allowed to describe the dynamic system during the filtration and backwash with satisfactory coefficient regression around 86%. The optimal backwash strategy consists of applying a filtration phase until reaching a singular arc corresponding to an optimal critical accumulated mass onto the membrane. To keep the mass around the singular arc the optimal strategy indicates that backwash should be performed more frequently with a filtration/backwash cycle times of 7.5 min/45s instead of 10 min/45s for the classical strategy. Compared with the classical backwash scheduling, the optimal strategy decreased the total resistance particularly the residual fouling of 14% and the energy pumping consumption of 7%.

The results of this study are very promising and have proven the effectiveness of mathematical tools to better control clogging. However, to apply these advanced optimization techniques on an industrial scale it would be interesting to extend this work to longer term operation. So as future work, an adaptative feedback control can be envisaged over longer term to continuously adjust the parameters of the model and thus rectify/adapt the optimal strategy if the filtration system is subjected to variability of influent quality, fouling degree or others various operating conditions.

## Acknowledgment

This study was financially supported by the research program (PEJC 12-06) of Ministry of Higher Education (Tunisia). This work was carried out with the collaboration of ONAS (National Sanitation Office, Tunisia). The authors like to thank ONAS team for their technical assistance, support and space allocation to install the MBR in WWTP of Charguia. Finally, the authors want to express their gratitude to Mr. Hamrouni for graciously providing them the Zenon MBR pilot. Authors thank the Euro-Mediterranean research TREASURE network (cf.www6.inrae.fr/treasure).

## Appendix

The optimal control synthesis for constant flux filtration system was developed in [25, 27] and is summarized in this Appendix.

**Optimal control Analysis**

The optimal control is defined as [27]:

$$\inf_{u(\cdot)} \int_0^{t_f} \left(E_+(m(t)) + u(t)E_-(m(t))\right)dt \qquad \text{A.1}$$

Subject to

$$\begin{cases} \dot{m} = f_-(x) + uf_+(x),\ m(0) = m_0 \\ \dot{V} = J_- + uJ_+,\ \mathrm{V}(0) = V_0 \end{cases} u \in [-1,1]$$

The process stops at the first time $t_f$ for which the target is reached: $V(t_f) = V^*$.

For convenience, $E_+$, $E_-$, $f_+$, $f_-$, $J_+$ and $J_-$ are defined as:

$$E_+(m) = \frac{E_f(m) + E_{BW}(m)}{2},\ E_-(m) = \frac{E_f(m) - E_{BW}(m)}{2}$$

$$f_+(x) = \frac{f_f(x) + f_{BW}(x)}{2},\ f_-(x) = \frac{f_f(x) - f_{BW}(x)}{2}$$

And

$$J_+ = \frac{J_v + J_{BW}}{2},\ J_- = \frac{J_v - J_{BW}}{2}$$

For simplicity the simple expressions of the functions $f_f, f_{BW}, E_f, E_{BW}$ are re written as:

$$f_f(m) = -a_p m + b_p,\ f_{BW}(m) = a_r m$$
$$E_f(m) = k_{1f}\mathrm{m} + k_{2f},\ E_{BW} = k_{1BW}m + k_{2BW}$$

where $a_p, b_p, a_r, k_{1f}, k_{2f}, k_{1BW}, k_{2BW}$ are non-negative parameters.

the Hamiltonian of the system is [27]:

$$H(m, \lambda_m, \lambda_V, u) = \lambda_m[f_-(m) + uf_+(m)] + \lambda_V[J_- + uJ_+] + \lambda_0[E_+(m) + uE_-(m)] \qquad \text{A.2}$$

where $\lambda_0$ is equal to -1 or 0. The Pontryagin's maximum principal states that for any optimal solution $u^\star(\cdot)$ there exists adjoint variables $\lambda_m(\cdot)$, $\lambda_V(\cdot)$ solutions of the adjoint system [27]

$$\begin{cases} \dot{\lambda}_m(t) = -\partial_m H(x(t), \lambda_m(t), \lambda_V(t), u^\star(t)) \\ \dot{\lambda}_V(t) = -\partial_V H(m(t), \lambda_m(t), \lambda_V(t), u^\star(t)) \end{cases}$$

Here, the adjoint equations are

$$\dot{\lambda}_m = -\lambda_m f_-'(m) - \lambda_0 E_+'(m) - u^\star(\lambda_m f_+'(m) + \lambda_0 E_-'(m))$$

$\dot{\lambda}_V = 0$

with the transversality conditions

$$\lambda_m(t_f) = 0,\ \lambda_V(t_f) \geq 0$$

From Eq. A.2, the switching function is

$$\phi(t) = \lambda_m(t) f_+(m(t)) + \lambda_V J_+ + \lambda_0 E_-(m(t))$$

which gives the following maximization conditions

$$u^\star(t) = \begin{cases} 1 & \text{when } \phi(t) > 0 \\ -1 & \text{when } \phi(t) < 0 \end{cases} \text{ a.e. } t \in [0, t_f]$$

For any optimal solution, one has the following properties [27]

i. $\lambda_0 = -1$ i.e. there does not exist abnormal extremal,

ii. there exists $\bar{t} < t_f$ such that $u^\star(t) = 1$ is optimal for $t \in [\bar{t}, t_f]$

iii. $\lambda_p$ is a positive constant.

**Singular arc**

A singular arc is possible only for constant values of $m$ equal to $\bar{m}$. Then, the corresponding value of the control for the trajectory to stay at $m = \bar{m}$ is

$$\bar{u} = -\frac{f_-(\bar{x})}{f_+(\bar{x})} = \frac{-(a_p + a_r)\bar{m} + b_p}{(a_r - a_p)\bar{m} + b_p} \qquad \text{A.3}$$

A straightforward computation gives

$$\dot{\phi} = \frac{1}{2}\left(a_r b_p \lambda_m + \left(a_r k_{1f} - a_p k_{1BW}\right)m + b_p k_{1BW}\right)$$

that can be written using the expression of $\phi$ as follows:

$$\dot{\phi} = \frac{a_r b_p}{(a_r - a_p)m + b_p}\phi + \psi(m, \lambda_V)$$

where the function $\psi$ has the expression

$$\psi(m, \lambda_V) = \frac{1}{2}\frac{M(m, \lambda_V)}{(a_r - a_p)m + b_p} \text{ with}$$
$$M(m, \lambda_V) = (a_p - a_r)(a_p k_{1BW} - a_r k_{1f})m^2 - 2(a_p k_{1BW} - a_r k_{1f})b_p m + a_r b_p(k_{2f} - k_{2BW} - 2\lambda_V J_+) + b_p^2 k_{1BW}$$

Therefore, a singular arc $x = \bar{x}$ has to satisfy

$$\Gamma(\bar{m}) = \psi\left(\bar{m}, \bar{\lambda}_V(\bar{m})\right) = 0$$

Finally, a straightforward but lengthy computation (verified with Maple) gives the following expression of Γ [27]

$$\Gamma(m) = -\frac{1}{2}\frac{N(m)}{\Delta(m)} \text{ with}$$
$$N(m) = -\left(a_r k_{1f} - a_p k_{1BW}\right)\left[\left(a_p J_{BW} + a_r J_v\right)m^2 - 2b_p J_{BW} m\right] + a_r b_p\left(k_{2f} J_{BW} + k_{2BW} J_v\right) + b_p^2 k_{1BW} J_{BW}$$

And

$$\Delta(m) = \left(a_p J_{BW} + a_r J_v\right)m - b_p J_{BW}$$

Consequently, a singular arc $m = \bar{m}$ is a root of $N$. And an arc $m = \bar{m}$ can be part of an optimal solution only if its corresponding adjoint $\bar{\lambda}_p(\bar{m})$ is positive.

The expression of $\bar{\lambda}_V$ is [27]:

$$\bar{\lambda}_V(x) = \frac{P_V(m)}{\Delta(m)}$$

with

$$P_V(m) = \left(a_r k_{1f} - a_p k_{1W}\right)m^2 + \left(a_r k_{2f} - a_p k_{2BW} + b_p k_{1BW}\right)x + b_p k_{2BW}$$

Finally, if an optimal solution possesses a singular arc, this imposes that the singular arc is left with $V = \bar{V}$ such that [27]:

$$\begin{aligned} \bar{V} &= V^\star - J_v \int_{\bar{m}}^{\bar{m}_f} \frac{dm}{f_f(m)} \\ &= V^\star - \begin{cases} \frac{J_v}{a_p}\log\left(\frac{-a_p\bar{m}+b_p}{-a_p\bar{m}_f+b_p}\right) \text{ if } a_p > 0 \\ \frac{J_v}{b_p}\left(\bar{m}_f - \bar{m}\right) \text{ if } a_p = 0 \end{cases} \end{aligned} \quad \text{A.4}$$

The final state $\bar{m}_f = m\left(t_f\right)$ satisfy the condition $\lambda_V J_v - E_f\left(\bar{m}_f\right) = 0$, thus

$$\bar{m}_f = \frac{\lambda_V(\bar{m})J_v - k_{2f}}{k_{1f}} \quad \text{A.5}$$

## References


[1] F. Zanetti, G. De Luca, R. Sacchetti, Performance of a full-scale membrane bioreactor system in treating municipal wastewater for reuse purposes, Bioresour Technol. 101 (2010) 3768–3771. https://doi.org/10.1016/j.biortech.2009.12.091.

[2] X. Du, Y. Shi, V. Jegatheesan, I.U. Haq, A Review on the Mechanism, Impacts and Control Methods of Membrane Fouling in MBR System, Membranes (Basel). 10 (2020) 24. https://doi.org/10.3390/membranes10020024.

[3] S.P. Hong, T.H. Bae, T.M. Tak, S. Hong, A. Randall, Fouling control in activated sludge submerged hollow fiber membrane bioreactors, Desalination. 143 (2002) 219–228. https://doi.org/10.1016/S0011-9164(02)00260-6.

[4] F. Meng, S. Zhang, Y. Oh, Z. Zhou, H.-S. Shin, S.-R. Chae, Fouling in membrane bioreactors: An updated review, Water Res. 114 (2017) 151–180. https://doi.org/10.1016/j.watres.2017.02.006.

[5] E. Akhondi, F. Wicaksana, A.G. Fane, Evaluation of fouling deposition, fouling reversibility and energy consumption of submerged hollow fiber membrane systems with periodic backwash, J Memb Sci. 452 (2014) 319–331. https://doi.org/10.1016/j.memsci.2013.10.031.

[6] K. Azis, S. Ntougias, P. Melidis, Fouling control, using various operating cleaning methods, applied on an MBR system through continuous TMP monitoring, Desalination Water Treat. 167 (2019) 343–350. https://doi.org/10.5004/dwt.2019.24609.

[7] P. Krzeminski, J.H.J.M. van der Graaf, J.B. van Lier, Specific energy consumption of membrane bioreactor (MBR) for sewage treatment, Water Science and Technology. 65 (2012) 380–392. https://doi.org/10.2166/wst.2012.861.

[8] O. Díaz, L. Vera, E. González, Optimization of the operating parameters in a membrane bioreactor operated in direct-flow mode by assessing threshold flux for compressibility, Chem Eng Sci. 274 (2023) 118675. https://doi.org/10.1016/j.ces.2023.118675.

[9] L. Vera, E. González, O. Díaz, S. Delgado, Application of a backwashing strategy based on transmembrane pressure set-point in a tertiary submerged membrane bioreactor, J Memb Sci. 470 (2014) 504–512. https://doi.org/10.1016/j.memsci.2014.07.069.

[10] Z. Yusuf, N. Abdul Wahab, S. Sahlan, Fouling control strategy for submerged membrane bioreactor filtration processes using aeration airflow, backwash, and relaxation: a review, Desalination Water Treat. 57 (2016) 17683–17695. https://doi.org/10.1080/19443994.2015.1086893.

[11] B. Zhang, G. Kotsalis, J. Khan, Z. Xiong, T. Igou, G. Lan, Y. Chen, Backwash sequence optimization of a pilot-scale ultrafiltration membrane system using data-driven modeling for parameter forecasting, J Memb Sci. 612 (2020) 118464. https://doi.org/10.1016/j.memsci.2020.118464.

[12] X. Shi, G. Tal, N.P. Hankins, V. Gitis, Fouling and cleaning of ultrafiltration membranes: A review, Journal of Water Process Engineering. 1 (2014) 121–138. https://doi.org/10.1016/j.jwpe.2014.04.003.

[13] P. Schoeberl, M. Brik, M. Bertoni, R. Braun, W. Fuchs, Optimization of operational parameters for a submerged membrane bioreactor treating dyehouse wastewater, Sep Purif Technol. 44 (2005) 61–68. https://doi.org/10.1016/j.seppur.2004.12.004.

[14] N.O. Yigit, G. Civelekoglu, I. Harman, H. Koseoglu, M. Kitis, Effects of various backwash scenarios on membrane fouling in a membrane bioreactor, Desalination. 237 (2009) 346–356. https://doi.org/10.1016/j.desal.2008.01.026.

[15] M. Raffin, E. Germain, S.J. Judd, Influence of backwashing, flux and temperature on microfiltration for wastewater reuse, Sep Purif Technol. 96 (2012) 147–153. https://doi.org/10.1016/j.seppur.2012.05.030.

[16] Z. Cui, J. Wang, H. Zhang, H.H. Ngo, H. Jia, W. Guo, F. Gao, G. Yang, D. Kang, Investigation of backwashing effectiveness in membrane bioreactor (MBR) based on different membrane fouling stages, Bioresour Technol. 269 (2018) 355–362. https://doi.org/10.1016/j.biortech.2018.08.111.

[17] Y. Ye, V. Chen, P. Le-Clech, Evolution of fouling deposition and removal on hollow fibre membrane during filtration with periodical backwash, Desalination. 283 (2011) 198–205. https://doi.org/10.1016/j.desal.2011.03.087.

[18] K.-J. Hwang, C.-S. Chan, K.-L. Tung, Effect of backwash on the performance of submerged membrane filtration, J Memb Sci. 330 (2009) 349–356. https://doi.org/10.1016/j.memsci.2009.01.012.

[19] E. González, O. Díaz, L. Vera, L.E. Rodríguez-Gómez, J. Rodríguez-Sevilla, Feedback control system for filtration optimisation based on a simple fouling model dynamically applied to membrane bioreactors, J Memb Sci. 552 (2018) 243–252. https://doi.org/10.1016/j.memsci.2018.02.007.

[20] G. Mannina, A. Cosenza, The fouling phenomenon in membrane bioreactors: Assessment of different strategies for energy saving, J Memb Sci. 444 (2013) 332–344. https://doi.org/10.1016/j.memsci.2013.05.047.

[21] N.G. Cogan, S. Chellam, A method for determining the optimal back-washing frequency and duration for dead-end microfiltration, J Memb Sci. 469 (2014) 410–417. https://doi.org/10.1016/j.memsci.2014.06.052.

[22] N.G. Cogan, J. Li, A.R. Badireddy, S. Chellam, Optimal backwashing in dead-end bacterial microfiltration with irreversible attachment mediated by extracellular polymeric substances production, J Memb Sci. 520 (2016) 337–344. https://doi.org/10.1016/j.memsci.2016.08.001.

[23] S. Gao, Z. Wang, T. Ren, Y. Zhang, A combined mechanism (the open pores-cake dissolution) model for describing the trans-membrane pressure (P(t)) reduction in the backwash process at a constant flow rate, J Environ Chem Eng. 9 (2021) 106871. https://doi.org/10.1016/j.jece.2021.106871.

[24] N. Kalboussi, J. Harmand, A. Rapaport, T. Bayen, F. Ellouze, N. Ben Amar, Optimal control of physical backwash strategy - towards the enhancement of membrane filtration process performance, J Memb Sci. 545 (2018) 38–48. https://doi.org/10.1016/j.memsci.2017.09.053.

[25] N. Kalboussi, A. Rapaport, T. Bayen, N. Ben Amar, F. Ellouze, J. Harmand, Optimal Control of Membrane-Filtration Systems, IEEE Trans Automat Contr. 64 (2019) 2128–2134. https://doi.org/10.1109/TAC.2018.2866638.

[26] N.G. Cogan, D. Ozturk, K. Ishida, J. Safarik, S. Chellam, Membrane aging effects on water recovery during full-scale potable reuse: Mathematical optimization of backwashing frequency for constant-flux microfiltration, Sep Purif Technol. 286 (2022) 120294. https://doi.org/10.1016/j.seppur.2021.120294.

[27] F. Aichouche, N. Kalboussi, A. Rapaport, J. Harmand, Modeling and optimal control for production-regeneration systems - preliminary results -, in: 2020 European Control Conference (ECC), IEEE, 2020: pp. 564–569. https://doi.org/10.23919/ECC51009.2020.9143741.

[28] Q. Liu, J. Ren, Y. Lu, X. Zhang, F.A. Roddick, L. Fan, Y. Wang, H. Yu, P. Yao, A review of the current in-situ fouling control strategies in MBR: Biological versus physicochemical, Journal of Industrial and Engineering Chemistry. 98 (2021) 42–59. https://doi.org/10.1016/j.jiec.2021.03.042.

[29] S. Judd, The MBR Book, Elsevier, 2006. https://doi.org/10.1016/B978-1-85617-481-7.X5000-4.

[30] P. Le Clech, B. Jefferson, I.S. Chang, S.J. Judd, Critical flux determination by the flux-step method in a submerged membrane bioreactor, J Memb Sci. 227 (2003) 81–93. https://doi.org/10.1016/j.memsci.2003.07.021.

[31] A. Charfi, J. Harmand, N. Ben Amar, A. Grasmick, M. Heran, Deposit membrane fouling: influence of specific cake layer resistance and tangential shear stresses, Water Science and Technology. 70 (2014) 40–46. https://doi.org/10.2166/wst.2014.186.

[32] S. Delgado, R. Villarroel, E. Gonzalez, M. Morales, Aerobic Membrane Bioreactor for Wastewater Treatment – Performance Under Substrate-Limited Conditions, in: Biomass - Detection, Production and Usage, InTech, 2011. https://doi.org/10.5772/17409.

[33] T. Jiang, M.D. Kennedy, W.G.J. van der Meer, P.A. Vanrolleghem, J.C. Schippers, The role of blocking and cake filtration in MBR fouling, Desalination. 157 (2003) 335–343. https://doi.org/10.1016/S0011-9164(03)00414-4.

[34] E. McAdam, S. Judd, Optimisation of dead-end filtration conditions for an immersed anoxic membrane bioreactor, J Memb Sci. 325 (2008) 940–946. https://doi.org/10.1016/j.memsci.2008.09.032.